

VALIDATION OF TWO-FLUID MODEL IN SHEAR-FREE MIXING LAYERS

Raad I. Issa

Imperial College of Science, Technology and Medicine
Department of Mechanical Engineering
London, SW7 2BX
England

Paulo J. Oliveira

Universidade da Beira Interior
Departamento de Engenharia Electromecânica
6200 Covilhã
Portugal

ABSTRACT

The paper presents the validation of an existing two-fluid model in the limiting case of dispersion of scalar concentration in a turbulent shear-free mixing-layer. The two phases in this case have identical physical properties and represent differently marked particles of the same fluid. The model (incorporated in a finite-volume numerical solution procedure) is applied to predict the dispersion rate of the scalar concentration, which has an initial step-profile and is then convected by grid-generated turbulence. The computations are compared with the exact solution to the scalar diffusion equation and with the measurements of Huq and Britter (1995). Very good agreement is obtained. The paper highlights which of the modelled terms in the equations are responsible for the dispersion effects and verify the correctness of the modelling assumptions.

1. INTRODUCTION

The two-fluid model provides a basis for the numerical prediction of two-phase flows in general. The derivation of the governing equations for such models involves an averaging process of some sort which results in terms requiring closure. These terms represent the interfacial forces as well as additional effects due to turbulence. Closure for these terms is provided by recourse to either empiricism or to approximate analysis of the local flow fields. Thus, the governing equations embody several assumptions the validity of which need verification.

Because the two-fluid model equations embody several complex effects arising in two-phase flows, it is

difficult to validate the different modelling assumptions individually against experiment. One flow case which can be used for such validation is that of the dispersion of scalar concentration in shear-free flow with nearly homogeneous turbulence; for this case, an analytic solution as well as experimental data exist. This is a simpler case than the shear/mixing-layer situation where variations in both concentration and velocity exist. There are a number of experimental studies for this latter case (see e.g. Fiedler *et al.* 1993) in contrast to the simpler case considered here which has received much less attention. Yet, it is the shear-free flow which enables the isolation of turbulence effects on phase dispersion. Even for the case of simple near-isotropic decaying turbulence behind a mesh, it is more common to find works where the imposed scalar profile at inlet has a constant gradient value (e.g. Sirivat and Warhaft, 1983, or Chasnov, 1993) as compared to the more complex stepwise scalar profile which is the interest of the present work. Data for this latter case were recently published by Huq and Britter (1995) and serve as a basis for comparison and assessment in the present study.

The paper presents the validation of an existing two-fluid model (Issa and Oliveira, 1993 and 1995) in the limiting case of dispersion of scalar concentration in a turbulent mixing-layer. The two phases in this case have identical physical properties and represent differently marked particles of the same fluid. The flow is planar in the mean and the velocity is uniform; two streams carrying different scalar concentrations are allowed to mix together in a field of grid-generated decaying turbulence. The model (incorporated in a finite-volume

numerical solution procedure) is applied to predict the dispersion rate of the scalar concentration due to turbulence. The computations are compared with the exact solution to the scalar diffusion equation and with the measurements of Huq and Britter (1995); very good agreement is obtained. The paper highlights which of the modelled terms in the equations are responsible for the dispersion effects and will verify the correctness of the modelling assumptions. In section 2, the equations are given and modelling assumptions outlined; departures from previous work are described in more detail. Section 3 summarises the numerical method. In section 4, the results of calculations are analysed and compared with both the analytical solution and the experimental data provided by Huq and Britter.

2. EQUATIONS AND TURBULENCE MODELLING

The transport equations comprising the two-fluid model utilised here are similar to those given in Issa and Oliveira (1995) which were derived following a volume-time averaging procedure. The continuity equation is:

$$\rho_k \left(\frac{\partial}{\partial t} \bar{\alpha}_k + \nabla \cdot \bar{\alpha}_k \tilde{\mathbf{u}}_k \right) = 0 \quad (1)$$

and the momentum equation:

$$\begin{aligned} \rho_k \left(\frac{\partial}{\partial t} \bar{\alpha}_k \tilde{\mathbf{u}}_k + \nabla \cdot \bar{\alpha}_k \tilde{\mathbf{u}}_k \tilde{\mathbf{u}}_k \right) = & -\bar{\alpha}_k \nabla \bar{p} + \bar{\alpha}_k \nabla \cdot \tilde{\boldsymbol{\tau}}_k \\ & + \nabla \cdot \bar{\alpha}_k \tilde{\boldsymbol{\tau}}_k^t + \rho_k \bar{\alpha}_k \tilde{\mathbf{g}} + \bar{\mathbf{F}}_{D_k} \end{aligned} \quad (2)$$

In these equations the main dependent variables are the phase averaged velocity $\tilde{\mathbf{u}}$, pressure \bar{p} , and the time averaged volume-fraction $\bar{\alpha}_k$, where the index k is a phase indicator ($k=c$ or d for the continuous or dispersed phase). The above equations are derived by an averaging process in which instantaneous variables such as velocity are decomposed into a phase-averaged mean ($\tilde{\mathbf{u}}$) plus phase fluctuation (\mathbf{u}''); these components are related to the unweighted mean velocity ($\bar{\mathbf{u}}$) and its fluctuation (\mathbf{u}') by:

$$\mathbf{u} = \bar{\mathbf{u}} + \mathbf{u}' = \tilde{\mathbf{u}} + \mathbf{u}'' \quad (3)$$

The phase average velocity is defined in a similar way as density average of Favre (1965) :

$$\tilde{\mathbf{u}} = \frac{\overline{\alpha \mathbf{u}}}{\bar{\alpha}} \quad (\text{implying } \overline{\alpha \mathbf{u}''} = 0). \quad (4)$$

A similar definition holds for the turbulent stress of each phase:

$$\tilde{\boldsymbol{\tau}}_k^t = - \frac{\rho_k \overline{(\alpha \mathbf{u}' \mathbf{u}')}_k}{\bar{\alpha}_k} \quad (5)$$

Turbulence modelling required for closure follows from an extension of the two-equation $k-\epsilon$ model to two phase flow (Gosman *et al.*, 1992, and Issa and Oliveira 1993, 1995), which results in transport equations for the turbulence kinetic energy of the continuous phase (\tilde{k}_c) and its dissipation rate ($\tilde{\epsilon}_c$):

$$\begin{aligned} \rho_c \left(\frac{\partial}{\partial t} \bar{\alpha}_c \tilde{k}_c + \nabla \cdot \bar{\alpha}_c \tilde{\mathbf{u}}_c \tilde{k}_c \right) = & \nabla \cdot \left(\bar{\alpha}_c \frac{\mu_c^t}{\sigma_k} \nabla \tilde{k}_c \right) + \\ & + \bar{\alpha}_c (G - \rho_c \tilde{\epsilon}_c) + S_d^k \end{aligned} \quad (6)$$

$$\begin{aligned} \rho_c \left(\frac{\partial}{\partial t} \bar{\alpha}_c \tilde{\epsilon}_c + \nabla \cdot \bar{\alpha}_c \tilde{\mathbf{u}}_c \tilde{\epsilon}_c \right) = & \nabla \cdot \left(\bar{\alpha}_c \frac{\mu_c^t}{\sigma_\epsilon} \nabla \tilde{\epsilon}_c \right) + \\ & + \bar{\alpha}_c \frac{\tilde{\epsilon}_c}{\tilde{k}_c} (C_1 G - C_2 \rho_c \tilde{\epsilon}_c) + S_d^\epsilon \end{aligned} \quad (7)$$

The continuous phase eddy viscosity is obtained as usual from $\nu_c^t = C_\mu \tilde{k}_c^2 / \tilde{\epsilon}_c$. The generation of \tilde{k} in Eq. (6) is given by $G = \mu_c^t \nabla \cdot \bar{\mathbf{u}}_c : (\nabla \bar{\mathbf{u}}_c + \nabla \bar{\mathbf{u}}_c^T)$ and the model constants are assigned standard values ($C_1=1.44$, $C_2=1.92$, $C_\mu=0.09$, $\sigma_k=1.0$, $\sigma_\epsilon=1.22$).

Closure is now required for the interphase momentum term (here assumed to result from drag only \mathbf{F}_D), for the phase turbulent stresses $\tilde{\boldsymbol{\tau}}_k$, and for the additional terms in the k and ϵ equations, S_d^k and S_d^ϵ respectively. Oliveira (1992) proposed the approximation $\alpha' \mathbf{u}' \mathbf{u}' / \bar{\alpha} \simeq \mathbf{u}'' \mathbf{u}''$ which leads to $\alpha (\mathbf{u}' \mathbf{u}') = \bar{\alpha} (\mathbf{u}' \mathbf{u}')$; thus $\tilde{\boldsymbol{\tau}}_k^t = \bar{\boldsymbol{\tau}}_k^t$ and $\tilde{k}_c = \bar{k}_c$, and the Boussinesq assumption can then be invoked:

$$\tilde{\boldsymbol{\tau}}_k^t = \mu_k^t (\nabla \bar{\mathbf{u}}_k + \nabla \bar{\mathbf{u}}_k^T) - \frac{2}{3} (\mu_k^t \nabla \cdot \bar{\mathbf{u}}_k + \rho_k \bar{k}_k) \delta \quad (8)$$

It should be noticed that this assumption departs from the common practice of setting $\tilde{\boldsymbol{\tau}}^t$ proportional to the rate of strain based on phase averaged velocities (i.e. $\tilde{\boldsymbol{\tau}}^t \propto \nabla \tilde{\mathbf{u}}$). For the present problem there are advantages in the form given above as it will be made clear further down. In general, since the main dependent variable in the momentum equation (2) is the $\tilde{\mathbf{u}}$ velocity, this must appear explicitly in the stress model above. With help of the relationship $\bar{\mathbf{u}} = \tilde{\mathbf{u}} + \mathbf{u}''$, Eq. (8) can be written in terms of the rate of strain of $\tilde{\mathbf{u}}$ plus additional terms (see Issa and Oliveira, 1995) and that is used to compute the continuous phase turbulent stress.

In order to compute the turbulent stress of the dispersed phase it is necessary to relate its turbulence kinetic energy and eddy viscosity to the respective continuous phase values by means of response functions:

$$C_k = \frac{\tilde{k}_d}{\tilde{k}_c} = \frac{\overline{\mathbf{u}'_d \cdot \mathbf{u}'_d}}{\overline{\mathbf{u}'_c \cdot \mathbf{u}'_c}} \quad (9)$$

$$C_\nu = \nu_d^t / \nu_c^t \quad (10)$$

In Issa and Oliveira (1995) the following forms have been proposed:

$$C_k = \frac{3 + \beta}{1 + \beta + 2\rho_d/\rho_c} \quad (\text{with } \beta = \frac{t_e}{t_p}(1 + 2\frac{\rho_d}{\rho_c})) \quad (11)$$

and, based on Csanady (1963) work, but accounting for both inertia and crossing-trajectories effects,

$$C_\nu = \left(1 + 0.45 \frac{\bar{u}_r^2}{C_k v_c^2}\right)^{-1/2} \quad (12)$$

where \bar{u}_r is the mean relative velocity ($\mathbf{u}_r = \mathbf{u}_d - \mathbf{u}_c$, $u_r = \sqrt{(\mathbf{u}_r \cdot \mathbf{u}_r)}$) and v is the root-mean square of \mathbf{u}' . In the present application these functions relating the response of particles to continuous phase turbulence are unity, because $\bar{u}_r = 0$ and $\rho_d = \rho_c$.

The drag force on the continuous phase resulting from interaction with a cloud of spherical particles is given by the expression:

$$\mathbf{F}_{D_c} = C_f \alpha_d \alpha_c (\mathbf{u}_d - \mathbf{u}_c) \quad (13)$$

which is valid at a given instant in time. In Eq. (13), $C_f \equiv (\frac{3}{4}\rho_c \bar{u}_r C_D)/d_p$ and the drag coefficient depends on the particle Reynolds number ($Re_p = \bar{u}_r d_p/\nu$) following a standard empirical formula: $C_D = (24/Re_p)(1 + 0.15 Re_p^{0.687})$. After time averaging and invoking the gradient diffusion hypothesis, $\alpha_c \mathbf{u}'_c = -\eta_c \nabla \bar{\alpha}_c$ where the scalar eddy diffusivity is given by $\eta_c = \nu_c^t/\sigma_\alpha$ (here $\sigma_\alpha = 0.7$), Eq. (13) results in:

$$\overline{\mathbf{F}_{D_c}} = C_f \left(\bar{\alpha}_d \bar{\alpha}_c (\bar{\mathbf{u}}_d - \bar{\mathbf{u}}_c) + (\bar{\alpha}_c \eta_c + \bar{\alpha}_d \eta_d) \nabla \bar{\alpha}_d - \overline{\alpha'_d \alpha'_d \mathbf{u}_r} \right) \quad (14)$$

The second term on r.h.s. of the above equation is referred to as the turbulent drag term and it is of great importance in the present problem as is the sole term that is responsible for dispersion. The full mean drag given by Eq. (14) can be derived from:

$$\overline{\mathbf{F}_{D_c}} = C_f \bar{\alpha}_d \bar{\alpha}_c (\bar{\mathbf{u}}_d - \bar{\mathbf{u}}_c) \quad (15)$$

by replacing $\bar{\mathbf{u}}$ with equivalent expressions in terms of $\bar{\mathbf{u}}$.

It is important at this point to discuss the significance of the drag term in the context of the pseudo two-phase flow case considered here. Since the two phases are nothing but part of the same fluid, with particles merely being marked differently, the drag term should vanish. This is indeed satisfied by Eq. (15) as $\bar{\mathbf{u}}_c$

becomes identical to $\bar{\mathbf{u}}_d$. However, the individual terms in Eq. (14), which is actually used to model $\overline{\mathbf{F}_{D_c}}$, are finite. In particular, the turbulent drag term represents the mechanism of dispersion and results in the $\bar{\mathbf{u}}_d$ field being different from that of $\bar{\mathbf{u}}_c$. But, these individual finite terms balance each other leading to the net effect of zero $\overline{\mathbf{F}_{D_c}}$. In this event, the magnitude of C_f is immaterial as it is multiplied by zero. Thus, the model is independent of the values used for the particle diameter or the drag coefficient C_D , as it should indeed be. This has been verified by carrying out computations with different values of d_p all of which yielded identical results.

The last terms to be considered are those appearing in the k and ϵ equations. In previous work (Issa and Oliveira, 1993), the dispersed-phase related turbulence energy source term S_d^k was approximated as:

$$S_d^k = -C_f \left(\eta_c (\bar{\mathbf{u}}_d - \bar{\mathbf{u}}_c) \cdot \nabla \bar{\alpha}_d + 2\bar{\alpha}_c \bar{\alpha}_d \tilde{k}_c (1 - C_i) \right) \quad (16)$$

where C_i represents an interaction response function analogous to C_k defined as:

$$C_i = \frac{\overline{\mathbf{u}'_c \cdot \mathbf{u}'_d}}{\overline{\mathbf{u}'_c \cdot \mathbf{u}'_c}} \quad (17)$$

which, from Tchen's work (cited by Hinze, 1975), is taken as $C_i = C_k$. In the present case, the precise form of C_i is not relevant since $C_k = 1$. However, the first term in the rhs of (16) requires attention. An important finding of this study was that the relative velocity in Eq. (16) could not be taken as the phase averaged value ($\bar{\mathbf{u}}_r = \bar{\mathbf{u}}_d - \bar{\mathbf{u}}_c$), but should instead be given by the relative mean value ($\bar{\mathbf{u}}_r = \bar{\mathbf{u}}_d - \bar{\mathbf{u}}_c$). This modification is justified in the following analysis, where the S_d^k term is re-derived. As done by Favre (1965), the instantaneous source term in the momentum Eq. (2) is multiplied by the phase velocity-fluctuation and then averaged:

$$S_d^k = \overline{(\mathbf{F}_{D_c} + \rho_c \alpha_c \mathbf{g}) \cdot \mathbf{u}''_c} = \overline{C_f \alpha_c \alpha_d (\mathbf{u}_d - \mathbf{u}_c) \cdot \mathbf{u}''_c} \\ \simeq C_f \bar{\alpha}_c \bar{\alpha}_d \bar{\mathbf{u}}_r \cdot \mathbf{u}''_c$$

Here the only approximations were to assume linear drag (C_f fluctuations are a second order effect) and to consider the dilute case ($\bar{\alpha}_c \simeq 1$). Introducing the phase averaged decomposition of the relative velocity ($\mathbf{u}_r = \bar{\mathbf{u}}_r + \mathbf{u}''_r$) into the last term above, leads to:

$$\overline{\alpha_d \mathbf{u}_r \cdot \mathbf{u}''_c} = \overline{\mathbf{u}''_c \cdot \bar{\mathbf{u}}_r} + \overline{\mathbf{u}''_c \cdot \mathbf{u}''_r} - \overline{\alpha_c \mathbf{u}''_c \cdot \mathbf{u}''_r}$$

which, by using the general relation $\mathbf{u}'' = \mathbf{u}' + \bar{\mathbf{u}}''$, can be developed to:

$$\overline{\alpha_d \mathbf{u}_r \cdot \mathbf{u}_c''} = \overline{\mathbf{u}_c'' \cdot \tilde{\mathbf{u}}_r} + \overline{\mathbf{u}_c' \cdot \mathbf{u}_r'} + \overline{\mathbf{u}_c'' \cdot \mathbf{u}_r''} - \overline{\alpha_c \mathbf{u}_c' \cdot \mathbf{u}_r'} - \overline{\alpha_c' \mathbf{u}_c' \cdot \mathbf{u}_r'} - \overline{\alpha_c \mathbf{u}_r' \cdot \mathbf{u}_c''}.$$

At this stage, the triple mean correlation $\overline{\alpha_c' \mathbf{u}_c' \cdot \mathbf{u}_r'}$ is neglected, the term $\overline{\mathbf{u}_c' \cdot \mathbf{u}_r'}$ is written explicitly in k_c with help of the C_i definition (17) (noting that $\tilde{k} = \bar{k}$), and all the other terms are easily modelled by means of gradient diffusion (because $\mathbf{u}'' = -\alpha' \nabla \alpha / \alpha \approx \eta \nabla \alpha / \alpha$; hence $\mathbf{u}_c'' = -\eta_c (\nabla \alpha_d) / \alpha_c$ and $\mathbf{u}_d'' = \eta_d (\nabla \alpha_d) / \alpha_d$). The mean relative velocity can be made to appear explicitly, since

$$\bar{\mathbf{u}}_r = \tilde{\mathbf{u}}_r + \overline{\mathbf{u}_r''} = \tilde{\mathbf{u}}_r + \frac{(\bar{\alpha}_c \eta_d + \bar{\alpha}_d \eta_c)}{\bar{\alpha}_c \bar{\alpha}_d} \nabla \bar{\alpha}_d \quad (18)$$

and the final modelled form for the drag-turbulence interaction term is:

$$S_d^k = -C_f \left(\eta_c \nabla \bar{\alpha}_d \cdot \bar{\mathbf{u}}_r + 2 \bar{\alpha}_c \bar{\alpha}_d \tilde{k}_c (1 - C_i) - \eta_c (\eta_c - \eta_d) \nabla \bar{\alpha}_d \cdot \nabla \bar{\alpha}_d \right) \quad (19)$$

Comparison of Eq. (16) with (19) shows that the mean relative velocity is now used instead of the phase averaged one. In previous applications the precise form for this term was not important since it tended to be very small (see Oliveira, 1992); this happened because the gradient of $\bar{\alpha}_d$ was small along the direction of the main slip, thus yielding a negligible product $\tilde{\mathbf{u}}_r \cdot \nabla \bar{\alpha}_d$. In the present application, since the two fluids are identical, the source term S_d^k should vanish. This does result from Eq. (19) since the relative velocity $\bar{\mathbf{u}}_r$ is zero, C_i is unity and $\eta_c = \eta_d$.

The source term in the k equation induces a dissipation equal to that term divided by the turbulence time scale (k/ϵ). Hence the additional source in the ϵ equation is modelled as:

$$S_d^\epsilon = -C_3 \frac{\tilde{\epsilon}_c}{k_c} 2C_f \bar{\alpha}_c \bar{\alpha}_d \tilde{k}_c (1 - C_i), \quad (20)$$

where the model constant C_3 is taken as unity in the absence of any knowledge of its actual magnitude.

3. NUMERICAL SOLUTION OF THE MODEL EQUATIONS

The averaged transport equations for momentum and mass of each phase, and for the turbulence kinetic energy and turbulence dissipation of the continuous phase, are solved by a finite-volume numerical method. The equations are discretised on a non-staggered mesh and the sets of discretised equations are solved iteratively in a sequential manner. The algorithm developed utilises

the pressure-correction technique extended to two-phase flow and applied in a time-marching fashion whereby the velocity, pressure and scalars at a new time level are computed from their values at the previous time level. It follows exactly the methodology described in detail by Issa and Oliveira (1993a). The computational meshes will be defined in section 5 and are non-uniform in both the streamwise and lateral directions so as to capture the sharp variation at the interface between the two different concentration layers. A second-order scheme, the linear-upwind differencing scheme (LUDS) has been adopted to discretise the convective terms in the equations, whereas the diffusive terms are discretised by the common central-differencing scheme.

4. APPLICATION AND RESULTS

The model is applied to the prediction of passive scalar dispersion in a homogeneous flow behind a grid. A theoretical solution for this problem is given below and experimental data were obtained by Huq and Britter (1995) who give a full description of the experimental set up, shown schematically in Fig. 1. It consists of two homogeneous fluid layers of equal density separated by a sharp interface ($y=0$) between different mean concentrations of the passive scalar. Both layers flow through a turbulence-generating grid ($x=0$) and the molecular diffusivity was varied in the experiment by using two different scalars, heat (molecular Schmidt number $\sigma=7$) and salt ($\sigma=700$). The mean axial velocity has been kept constant, $U=7.7$ cm/s, yielding a Reynolds number based on the mesh spacing ($M=3.2$ cm) of $Re_M \approx 2500$.

The analytic solution to the above described flow is governed by the transport equation:

$$U \frac{\partial \alpha}{\partial x} = \eta \frac{\partial^2 \alpha}{\partial y^2} \quad (21)$$

where U is the uniform streamwise velocity, η is the eddy-diffusivity (assumed to be much larger than the molecular diffusivity) and α is the concentration. The above equation is subject to the boundary conditions:

- $x=0$: $\alpha = \alpha_1$ for $y > 0$ and $\alpha = \alpha_2$ for $y \leq 0$
 - $x > 0$: $\alpha = \alpha_1$ for $y \rightarrow \infty$ and $\alpha = \alpha_2$ for $y \rightarrow -\infty$
- The solution to this Cauchy problem is obtained by Fourier transform and can be shown to be:

$$\alpha(x,y) \equiv \frac{\bar{\alpha}_d - \alpha_1}{\alpha_2 - \alpha_1} = \frac{1}{2} \operatorname{erfc} \left(\frac{\sqrt{\pi} y}{2 \bar{h}} \right) \quad (22)$$

where \bar{h} is the half-width of the concentration profile and is obtained from:

$$\bar{h} \equiv 1 / (2 \frac{\partial \alpha}{\partial y})_{y=0} = \sqrt{\frac{\pi \eta x}{U}}. \quad (23)$$

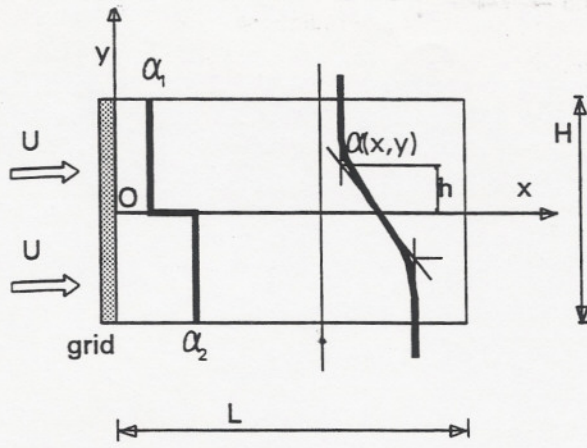


Fig. 1 Sketch of the flow configuration

This problem has been simulated numerically as a two phase flow in the rectangular two-dimensional x-y domain of Fig. 1, the two phases consisting of the same fluid (with density $\rho_c = \rho_d = \rho$ and viscosity $\mu_c = \mu_d = \mu$). The second (dispersed) phase is distinguished from the other by marking its fluid particles with a different volume concentration $\bar{\alpha}_d \ll \bar{\alpha}_c$. The following boundary conditions have been imposed:

- inlet at $x=0$, where $\bar{u}_c = \bar{u}_d = U$, $k_c = k_{in}$, $\epsilon_c = \epsilon_{in}$ and $\bar{\alpha}_d = \alpha_2$ (for $y \leq 0$), $\bar{\alpha}_d = \alpha_1$ (for $y > 0$)
- outlet at $x=L$, with the usual zero-gradient conditions ($\partial/\partial x \equiv 0$)
- symmetry planes at $y = \pm H/2$ with no normal fluxes for each phase and zero-gradient conditions ($\partial/\partial y \equiv 0$).

Initial checks were done to assess the adequacy of the computational mesh and the truncation error associated with the differencing scheme. Most calculations were done in a mesh with 50×40 control-volumes along the streamwise and transverse directions, respectively. This mesh has non-uniform spacing, with points concentrated close to the center-line ($y=0$), so as to resolve properly the lateral profiles of concentration which possess steeper gradients at $y=0$. Points were also concentrated near the turbulence-generating grid ($x=0$), where the imposed step profile of α tends to change very rapidly to a smooth profile which then evolves with the streamwise distance x .

To establish grid-independence of the solution, calculations were made with the first order upwind difference scheme (UDS), as well as the second order linear upwind scheme (LUDS). A comparison of predictions based on UDS and LUDS is shown in Fig. 2 for an α -profile not far from the inlet (at $x = 16$ mm), where the lateral gradients are still quite steep. The two curves are almost indistinguishable in the figure, with

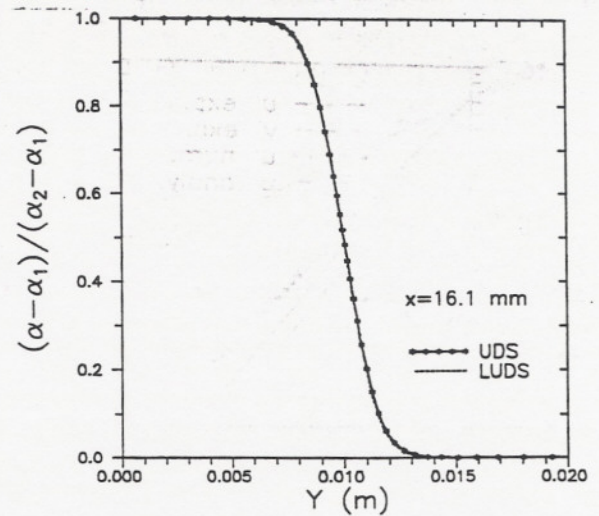


Fig. 2 Predicted profiles of concentration using 2 differencing schemes

LUDS giving a slightly sharper gradient. This verifies that the mesh used is fine enough to give accurate solutions.

Since dispersion is brought about by fluid turbulence, it is pertinent to assess how the model predicts some of the turbulence characteristics. Huq and Britter (1995) correlated their velocity fluctuation data by the relations $(u'_i/U)^2 = A(x/M - 4)^{-1.4}$, with $A = 0.07$ for u' and 0.05 for v' . In Fig. 3 these experimental curves are compared with the numerical predictions. Since the k - ϵ model is an isotropic model, it cannot distinguish the longitudinal from the lateral fluctuation, both are given by $u' = \sqrt{2/3}k$. In the predictions in Fig. 3 the inlet was taken at $x/M - 4 = 1$ and the corresponding values of k and ϵ were set according to the data; it is seen that the predicted decay of k follows closely the data for u' having however a somewhat different decay rate. This is not surprising, since the k and ϵ equations for homogeneous, isotropic, decaying turbulence reduce to $\partial k/\partial t = -\epsilon$ and $\partial \epsilon/\partial t = -C_2 \epsilon^2/k$, with solution $k/k_0 = (1 + (C_2 - 1)\epsilon_0 t/k_0)^{-1/(C_2 - 1)}$ where k_0 and ϵ_0 are the initial values. This solution, with $t = x/U$, is also plotted in Fig. 3 as the analytical curve, and is almost coincident with the numerical prediction (the difference may be due to some diffusion of k not considered in the analytic solution). In conclusion, the asymptotic coefficient of decay is $1/(C_2 - 1) = 1.09$ for the k - ϵ model and 1.4 for the experimental data; this difference explains the different rates seen in Fig. 3.

The main purpose of the paper is demonstrate that the two-fluid model presented above can predict scalar dispersion. This can be done by comparing predicted

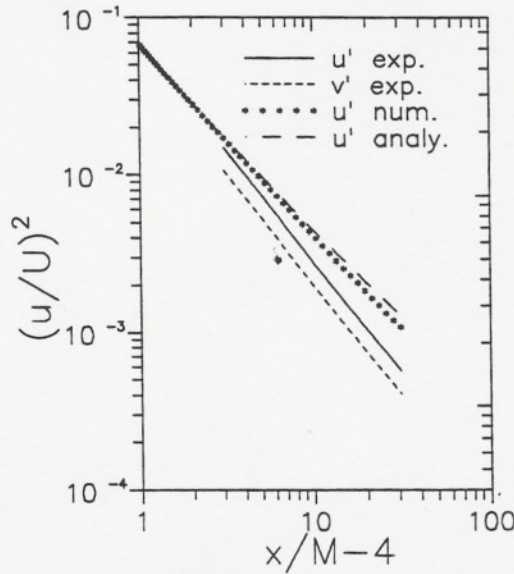


Fig. 3 Streamwise decay of mean-square turbulence fluctuations. Experimental data of Huq & Britter, 1995.

lateral profiles of the mean scalar (here, the volume-fraction α), at several axial locations, with the data of Huq and Britter (1995). However, since the values of k and ϵ at the location of the turbulence-generating grid (where the step profile for α is valid) are not known from the experiments, the comparison has to be done in terms of non-dimensional values. In figure 5 of Huq and Britter (1995) it is shown that the experimental points for their mean scalar follow an error function when the distances x and y are non-dimensionalised by the layer half-width, \bar{h} , and that this self-similarity agreement improves with increasing x . A check that the numerical predictions follow the same curve ($C/\Delta C = \frac{1}{2} \text{erfc}(z/\bar{h})$ in Huq and Britter), can be made by reference to Fig. 4 where prediction at several x stations are compared with the analytic curve. As can be observed, the predicted profiles collapse into a single curve (only a few points at the first station are slightly off the trend, probably due to inlet effects) but this curve does not follow closely the error function. Explanation for this discrepancy follows from the theoretical solution given above: the argument of the error-function should be $(y\sqrt{\pi})/(2\bar{h})$ and not y/\bar{h} . When the numerical results are re-plotted with that scale, in Fig. 5, the agreement between numerical predictions and theory is very good. The figure also confirms that there is good agreement between predictions and the experimental data of Huq and Britter.

Additional confirmation of the appropriateness of the model for this problem is shown in Fig. 6, where the

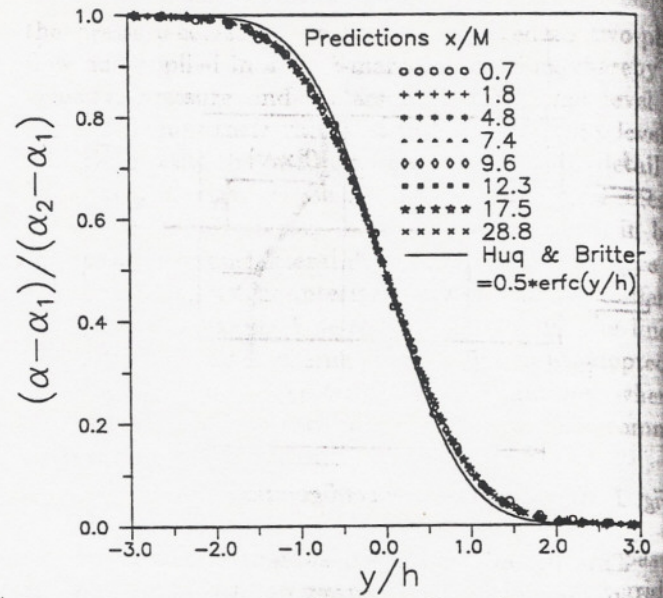


Fig. 4 Comparison of predicted profiles of concentration at several axial positions and the theoretical curve given by Huq & Britter ($\alpha = 0.5\text{erfc}(y/\bar{h})$)

mean half-width, \bar{h} , is plotted against the streamwise distance, x . The evolution of \bar{h} in this figure represents the rate of dispersion of the scalar α by lateral turbulent fluxes $\alpha v'$, and according to the analytical solution, \bar{h} should grow as $x^{1/2}$ (see Eq. (23)). The agreement seen in Fig. 6 between the curve with slope $1/2$ and the numerical prediction of \bar{h} ($\bar{h} = 1/(2\Delta_j \alpha/\Delta_j y)$) is remarkable.

The perfect agreement between predictions and analytical solution in Fig. 5 means that the two-fluid model of section 2 can accurately capture a convection-diffusion equation like (21). When the two-fluid model is formulated in terms of time-averaged quantities, such an equation arises naturally in the continuity equation, from the correlation $\alpha u'$ (see e.g. Elghobashi and Abou-Arab 1983). In what follows it will be shown that within the phase-averaged formulation, an equivalent diffusion effect arises from the turbulent drag term in Eq. (14). The present problem could be solved with the single-phase flow equations, which simply result in $\bar{u}_c = U$ (constant), $\bar{v}_c = 0$, and a positive pressure gradient which compensates the decay of k , $dp(x)/dx = -\frac{2}{3}\rho_c dk/dx$. When some of the fluid particles are marked with a passive scalar, the mean and fluctuating velocity fields remain unchanged, thus $\bar{u}_c = \bar{u}_d = U$ and $u'_c = u'_d$. This last condition could also be obtained from the C_k formulation given by Eq. (11) which for $\rho_c = \rho_d$ yields $C_k = 1$; thus $k_d = k_c$, because $\bar{k} = k$. The interaction function C_i is equal to unity from its definition (17). Since there is no mean slip,

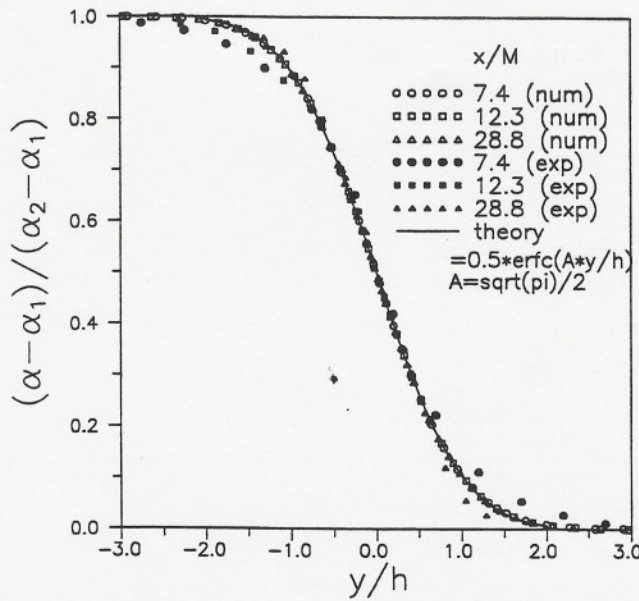


Fig. 5 Profiles of mean scalar concentration in self-similar form: comparison of predicted and measured (Huq & Britter) values, and the analytic solution ($\alpha = 0.5 \operatorname{erfc}(\sqrt{\pi} y / 2h)$)

which implies no crossing-trajectories effect, the Csanady-type C_v -function (12) becomes also unity, and so the two eddy viscosities are identical, $\nu_d^t = \nu_c^t$. From these considerations, and because in the model for the turbulent stresses given by Eq. (8) the strains are in terms of time-mean velocities, it results that $\tilde{\tau}_d^t = \tilde{\tau}_c^t$ and these are identically zero for the velocity field in question. The gravity term in the momentum Eqs. (2) can be incorporated into the pressure gradient since the two densities are identical. Hence the momentum equations reduce to the simple statement $\bar{u}_r = \tilde{u}_r + \bar{u}_r'' = 0$, which means that there is no mean drag between the 'phases'. It should be noted however that the precise drag factor C_f used is unimportant, since it appears as a multiplicative factor on the mean slip velocity (this means that the results are independent on the assumed particle diameter appearing in C_f). From (18), the statement $\bar{u}_r = 0$ becomes $\bar{\alpha}_d \tilde{u}_d - \bar{\alpha}_d \tilde{u}_c \approx -\eta \nabla \bar{\alpha}_d$, where the dilute flow approximation is used, $\bar{\alpha}_c \approx 1$ ($\Rightarrow \tilde{u}_c \approx \bar{u}_c$). After application of the nabla operator to this relation and using the continuity equations (1), it results in $\bar{u}_c \cdot \nabla \bar{\alpha}_d = \nabla \cdot \eta \nabla \bar{\alpha}_d$. For the present problem \bar{u}_c is aligned with x , the eddy diffusivity is known to be approximately constant, and the main gradients of α are in the lateral direction y ; thus, the convection-diffusion equation (21) is recovered.

5. CONCLUSIONS

Predictions of scalar dispersion in a fictitious two-

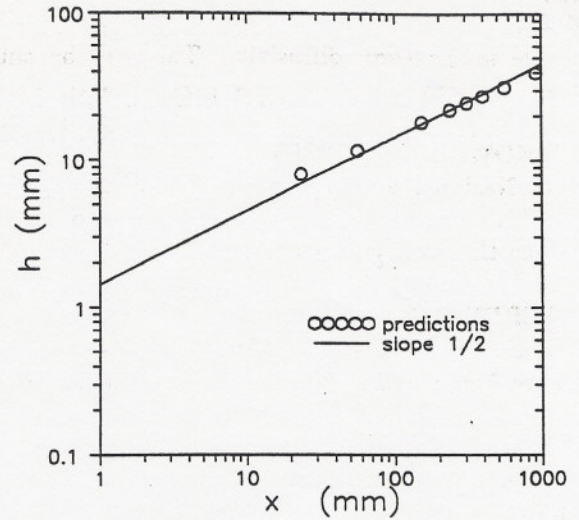


Fig. 6 Predicted axial variation of the layer half-width and theoretical curve

phase homogeneous flow behind a turbulence-generating mesh are made using the two-fluid model. At inlet, a step profile of the dispersed phase volume fraction is imposed thus marking the fictitious second phase. The governing equations are expressed in terms of phase averaged velocities and are solved by a finite-volume procedure. Turbulence of the continuous and the dispersed phases, which is the driving force for dispersion, is accounted for by an extension of the $k-\epsilon$ model.

The continuous phase turbulent stresses are modelled by the eddy viscosity assumption in terms of gradients of the un-weighted velocities, while turbulence of the dispersed phase is accounted for by appropriate response functions. For this case, the particle response function relating the turbulence kinetic energy of the dispersed phase to that of the continuous phase is unity since the two phases have identical physical properties. Similarly, the eddy viscosities of the dispersed and continuous phases are equal to each other because there is no inertia and crossing-trajectories effects. Profiles of predicted volume-fraction using the full two-fluid model are compared with a theoretical solution, which is here given. There is perfect agreement, demonstrating that for this case the two-fluid model reduces to a convection-diffusion equation.

Comparisons are also made with the data of Huq and Britter, demonstrating that the present model can predict well the mean scalar dispersion. Since the turbulence quantities at the grid, where the scalar profile has the stepwise shape, are not known from the experiment, it has not been possible to compare profiles of α in dimensional form and thus assess the values used

for the scalar eddy diffusivity. This will be subject to future research.

ACKNOWLEDGEMENTS

Junta Nacional de Investigação Científica e Tecnológica (JNICT, Portugal) is gratefully acknowledged for funding this work under project PBIC/C/CEG/2430/95.

REFERENCES

- Chasnov, J.R., 1993, "Decaying Turbulence in a Passive Mean Scalar Gradient", *Applied Sci. Res.*, Vol. 51, pp. 313-317.
- Csanady, G.T., 1963, "Turbulent Diffusion of Heavy Particles in the Atmosphere", *J. Atm. Sci.*, Vol. 20, pp. 201-208.
- Elghobashi, S.E., and Abou-Arab, T.W., 1983, "A Two-Equation Turbulence Model for Two-Phase Flows", *Phys. of Fluids*, Vol. 26, pp. 931-938.
- Favre, A., 1965, "Equations des Gazs Turbulents Compressibles", *J. de Mecanique*, Vol. 4, pp. 361-421.
- Fiedler, H.E., Lummer, M., and Nottmeyer, K., 1993, "Plane Mixing Layer Between Parallel Streams of Different Velocities and Different Densities", *Adv. in Turbulence Studies*, in *Progress in Astron. and Aeron.* AIAA., Vol. 149, Ed. H. Branover, pp. 40-52.
- Gosman, A.D, Lekakou, C., Politis, S., Issa, R.I., and Looney, M.K., 1992, "Multidimensional Modelling of Turbulent Two-Phase Flows in Stirred Vessels", *AIChE J.*, Vol. 38, p. 1946.
- Hinze, J.O., 1975, "Turbulence", 2nd edition, MacGraw-Hill.
- Huq, P., and Britter, R.E., 1995, "Mixing due to Grid-Generated Turbulence of a Two-Layer Scalar Profile", *J. Fluid Mech.*, Vol. 285, pp. 17-40.
- Issa, R.I., and Oliveira, P.J., 1993a, "Numerical Prediction of Phase Separation in Two-Phase Flow Through T-Junctions", *Computers and Fluids*, Vol. 23, pp. 347-372.
- Issa, R.I., and Oliveira, P.J., 1993, "Modelling of Turbulent Dispersion in Two Phase Flow Jets", *Turbulence Modelling and Experiment 2*, Elsevier, pp. 947-957.
- Issa, R.I., and Oliveira, P.J., 1995, "Numerical Prediction of Turbulent Dispersion in Two-Phase Jet Flows", *Proc. Int. Symp. on Two-Phase Flow Modelling and Experimentation*, Rome.
- Oliveira, P.J., 1992, "Computer Modelling of Multidimensional Multiphase Flow and Application to T-Junctions", Ph.D. Thesis, Imperial College, Univ. of London.
- Sirivat, A., and Warhaft, Z., 1983, "The Effect of a Passive Cross-Stream Temperature Gradient on the Evolution of Temperature Variance and Heat Flux in Grid Turbulence", *J. Fluid Mech.*, Vol. 128, pp. 323-346.